THE JOURNAL OF BIOLOGICAL CHEMISTRY VOL. 287, NO. 44, pp. 37383–37394, October 26, 2012

Prostaglandin H Synthase-2-catalyzed Oxygenation of 2-Arachidonoylglycerol Is More Sensitive to Peroxide Tone than Oxygenation of Arachidonic Acid*

Received for publication, May 12, 2012, and in revised form, August 12, 2012 Published, JBC Papers in Press, September 1, 2012, DOI 10.1074/jbc.M112.381202

Joel Musee and Lawrence J. Marnett[1]

From the A. B. Hancock Jr. Memorial Laboratory for Cancer Research, Departments of Biochemistry, Chemistry, and Pharmacology, Vanderbilt Institute of Chemical Biology, Center in Molecular Toxicology, and Vanderbilt-Ingram Cancer Center, Vanderbilt University School of Medicine, Nashville, Tennessee 37232-0146

Background: Prostaglandin H synthase-2 (PGHS-2)-mediated oxygenation of 2-arachidonoylglycerol (2-AG) produces prostaglandin glyceryl esters and modulates endocannabinoid tone.
Results: Oxygenation of 2-AG is more dependent on peroxide tone than is oxygenation of arachidonic acid (AA).
Conclusion: Endocannabinoid oxygenation by PGHS-2 is sensitive to peroxide tone.
Significance: Cellular redox status may be a factor in endocannabinoid oxygenation by PGHS-2.

The endocannabinoid, 2-arachidonoylglycerol (2-AG), is a selective substrate for the inducible isoform of prostaglandin H synthase (PGHS), PGHS-2. Its turnover leads to the formation of glyceryl esters of prostaglandins (PG-Gs), a subset of which elicits agonism at unique, as yet unidentified, receptors. The k_{cat}/K_m values for oxygenation of arachidonic acid (AA) and 2-AG by PGHS-2 are very similar, but the sensitivities of the two substrates to peroxide-dependent activation have not been compared. 15-Hydroperoxy derivatives of AA and 2-AG were found to be comparable in their ability to serve as substrates for the peroxidase activities of PGHS-2, PGHS-1, and glutathione peroxidase (GPx). They also were comparable in the activation of AA oxygenation by cyanide-inhibited PGHS-2. However, oxygenation of 2-AG was significantly suppressed relative to AA by the presence of GPx and GSH. Furthermore, 2-AG oxygenation by peroxidase-deficient H388YmPGHS-2 was much less efficient than AA oxygenation. Wild-type rates of 2-AG oxygenation were restored by treatment of H388YmPGHS-2 with hydroperoxide derivatives of AA or 2-AG. RNAi silencing of phospholipid hydroperoxide-specific GPx (GPx4) in NIH/3T3 cells led to increases in cellular peroxidation and in the levels of the isoprostane product, 8-epi-$PGF_{2\alpha}$. GPx4 silencing led to 2–4-fold increases in PG-G formation but no change in PG formation. Thus, cellular peroxide tone may be an important determinant of the extent of endocannabinoid oxygenation by PGHS-2.

Prostaglandin H synthases (PGHSs)[2] catalyze the first two steps in the biosynthesis of prostaglandins (PGs), a class of bioactive lipids that regulate a broad range of physiological responses. The cyclooxygenase activity of PGHSs oxygenates arachidonic acid (AA) (1) to the hydroperoxy endoperoxide, PGG_2, and the peroxidase activity reduces PGG_2 to PGH_2 (Fig. 1*A*). The two isoforms of PGHS, PGHS-1 and PGHS-2, are distinguished by different patterns of expression. In general, PGHS-1 is constitutive in tissues in which it is expressed, suggesting a homeostatic role, whereas PGHS-2 is inducible by a variety of inflammatory and proliferative stimuli (cytokines, bacterial lipopolysaccharide, growth factors, and tumor promoters), consistent with a role for PGs produced by this isoform in inflammation and cell proliferation (2). In addition to differences in regulation, PGHS enzymes exhibit biochemical differences related to their structures. These include the increased sensitivity of PGHS-2 to peroxide activation (3) and the presence of a sequence in PGHS-2 that renders it susceptible to cellular proteolysis (4). PGHS-2 also displays broader substrate specificity than PGHS-1. For example, it oxygenates ester and amide derivatives of AA much more efficiently than PGHS-1 (4). 2-Arachidonoylglycerol (2-AG) and arachidonoylethanolamide are of particular interest as PGHS-2 substrates because they occur in human tissue and are endogenous ligands for the cannabinoid receptors (CB_1 and CB_2) (5, 6).

PGHS-2-dependent oxygenation of 2-AG yields the glyceryl ester of PGH_2 (PGH_2-G). PGH_2-G is converted to a similar array of prostanoids as PGH_2 with the exception of its poor conversion to thromboxane A_2 glyceryl ester (7). Murine resident peritoneal macrophages stimulated with an inflammatory agonist (zymosan) produce both PGE_2-G and PGI_2-G (8), and PGD_2-G formation is elicited from the RAW264.7 macrophage-like cell line upon pretreatment with LPS and IFNγ followed by ionomycin (7). PGE_2-G has been isolated from rat

* This work was supported, in whole or in part, by National Institutes of Health Research Grant GM15431. This work was also supported by Vanderbilt Medical-Scientist Training Program Grant GM07347.
[1] To whom correspondence should be addressed: Dept. of Biochemistry, Vanderbilt University School of Medicine, 2200 Pierce Ave., Nashville, TN 37232-0146. Tel.: 615-343-7329; Fax: 615-343-7534; E-mail: larry.marnett@vanderbilt.edu.
[2] The abbreviations used are: PGHS, prostaglandin H synthase; AA, arachidonic acid; ABTS, 2,2′-azinobis(3-ethylbenzothiazoline-6-sulfonic acid; 2-AG, 2-arachidonoylglycerol; BODIPY, boron-dipyrromethene; GPx, glutathione peroxidase; GSSG, oxidized glutathione; GSSG reductase, glutathione reductase; h, human; 15-HpETE, 15-hydroperoxy-5*Z*,8*Z*,11*Z*,13*E*-eicosatetraenoic acid; 15-HpETE-G, 15-HpETE glyceryl ester; LC-ESI/MS/MS, liquid chromatography-electrospray ionization/tandem mass spectrometry; m, mouse; o, ovine; PG, prostaglandin; PG-G, prostaglandin glyceryl ester; PGH_2-G, PGH_2 glyceryl ester.

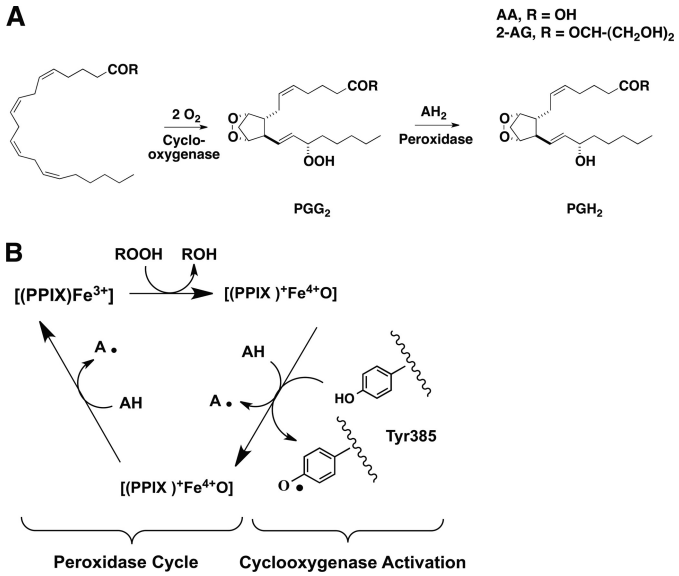

FIGURE 1. **Endoperoxide intermediates of fatty acyl substrate oxygenation by PGHS-2 (*A*) and the branched-chain mechanism (*B*).** *A*, the cyclooxygenase activity of PGHS *bis*-dioxygenates fatty acyl substrates (R → OH = AA, glycerol = 2-AG) leading to the formation of the endohydroperoxide PGG_2, which is reduced by the peroxidase activity to PGH_2 (or its glyceryl ester). *B*, schematic representation of the mechanism linking the peroxidase and cyclooxygenase activities of PGHS.

footpads in the presence and absence of an inflammatory stimulus (9). Thus, PG-Gs are produced by intact cells treated with a variety of stimuli and are present *in vivo*. The physiological relevance of PGHS-2-dependent 2-AG oxygenation is the subject of ongoing investigation. It is interesting to note that in cells, PGs are generated at far higher levels than PG-Gs following challenge with inflammatory stimuli. In the case of murine macrophages, this is partly due to a 10-fold difference in the concentrations of AA and 2-AG released in response to zymosan stimulation (8).

The k_{cat} values for oxygenation of AA and 2-AG by hPGHS-2 are comparable, whereas the k_{cat} for oxygenation of AA by mPGHS-2 is approximately twice that of 2-AG (10). An important property of oxygenated derivatives of 2-AG that has not been explored is the ability of glyceryl-hydroperoxides such as PGG_2-G to interact with the peroxidase activity of PGHS, either as substrates for peroxidatic reduction or as activators of the cyclooxygenase activity (Fig. 1*B*). Purified PGHS enzymes require hydroperoxide-dependent activation to become functional oxygenases. Fatty acid hydroperoxides, PG hydroperoxides, or peroxynitrite react with the heme prosthetic group (Fig. 1*B*) to produce a ferryl-oxo complex that oxidizes Tyr-385 in the oxygenase active site to produce a tyrosyl radical (Fig. 1*B*); the tyrosyl radical oxidizes the fatty acid substrate and is regenerated during the reaction cycle (2).

We have undertaken a study of the ability of glyceryl ester hydroperoxides compared with fatty acid hydroperoxides to serve as substrates for the peroxidase activities of PGHS-1 and PGHS-2, and to activate oxygenation by both enzymes. We also investigated the peroxide-dependent activation of AA and 2-AG oxygenation by PGHS-2 by conducting experiments that lowered peroxide tone *in vitro*. The results reveal a major difference in the sensitivity of PGHS-2 with respect to the oxygenation of the two substrates, specifically with regard to the concentration of peroxide required to activate the cyclooxygenase functionality. We also demonstrate that silencing of the phospholipid hydroperoxide-specific glutathione peroxidase (GPx4) in murine 3T3 fibroblasts leads to significant increases in PG-G formation (2–4-fold over control), with little to no increase in PG formation. Altogether, these results indicate that the peroxidase active site may represent an important site of the regulation of PGHS-2-mediated oxygenation of 2-AG.

EXPERIMENTAL PROCEDURES

Materials—AA, 2-AG, and hematin were obtained from Nu Chek Prep (Elysian, MN), Cayman Chemicals (Ann Arbor, MI), and Frontier Scientific (Logan, UT), respectively. All other reagents were from Sigma-Aldrich.

Enzymes—Purified bovine erythrocyte GPx and purified *Saccharomyces cerevesiae* glutathione reductase (GSSG reductase) were obtained from Sigma-Aldrich. Purified soybean 15-lipoxygenase was from Cayman Chemicals. hPGHS-2 and mPGHS-2 were expressed and purified as described (11). Site-directed mutagenesis to generate H388Y mPGHS-2 and subsequent expression and purification of the protein were performed as published (12). oPGHS-1 was purified from ram seminal vesicles (Oxford Biomedical Research, Oxford, MI), as described previously (13). The specific activities of hPGHS-2 and mPGHS-2 were both 62 μmol of AA/μmol of enzyme; the specific activity of oPGHS-1 was 325 μmol of AA/μmol of enzyme, and that of H388Y mPGHS-2 was 31 μmol of AA/μmol of enzyme.

Chemistry—15-Hydroperoxy-5*Z*,8*Z*,11*Z*,13*E*-eicosatetraenoic acid (15-HpETE) was generated with 40% yield as determined by UV spectroscopy (236 nm) using the molar absorptivity of the conjugated diene (ϵ_{236} = 29,500 $M^{-1}\cdot cm^{-1}$) (14). 15-HpETE glyceryl ester (15-HpETE-G) was generated as described (15) with minor modifications. Briefly, to 200 ml of oxygen-saturated 100 mM sodium borate buffer (pH 9.0) was added 750,000 units/ml purified soybean 15-lipoxygenase. 2-AG (25 mg in 2 ml of acetonitrile) was added to the buffer with continued perfusion of O_2 over the surface of the buffer and stirring. An aliquot of the reaction mixture was monitored by UV spectroscopy (236 nm) until no further increase in absorbance was evident (~10 min). The reaction mixture was extracted twice with 200 ml of diethyl ether, and the combined organic layers were dried using $MgSO_4$, filtered, and concentrated under vacuum. The residue was resuspended in acetonitrile and filtered over glass wool. Yield (30%) was determined using UV spectroscopy (236 nm). No further steps were carried out to purify the product. Purity was determined by HPLC/UV to be ≥95%.

The positions of hydroperoxide attachment were assigned by diagnostic fragmentation using collision-induced dissociation under the following liquid chromatography-electrospray ionization/tandem mass spectrometry (LC-ESI/MS/MS) conditions: a Phenomenex Luna C18 column (100 mm × 2.0 mm, 3 μm) was held at 40 °C and eluted isocratically with 40% A (5 mM NH_4OAc in H_2O):60% B (5 mM NH_4OAc in 90% CH_3CN) at 0.3 ml/min. Mass spectra were obtained on a ThermoFinnigan Quantum triple-quadrupole instrument equipped with an elec-

trospray source and operated in negative ion mode for 15-HpETE (ESI-MS *m/z* calculated for $C_{20}H_{32}O_4$ (M^-), 335.23; found 335.11) and in positive-ion mode for 15-HpETE-G (ESI-MS *m/z* calculated for $C_{23}H_{38}O_6$ ($M+NH_4^+$), 428.30; found 428.14) (ThermoFinnigan, San Jose, CA). Collision-induced dissociation fragmentation patterns were compared with those of authentic standards for both molecules with final confirmation of hydroperoxide regiochemistry of 15-HpETE and 15-HpETE-G by ^{1}H NMR.

15-HpETE ^{1}H NMR at 500 MHz ($CDCl_3$): 6.58–6.63 (dd, 1H, J = 11.1, 15.3 Hz CH), 5.98–6.02 (t, 1H, J = 10.9 Hz CH), 5.56–5.61 (dd, 1H, J = 7.85, 15.3 Hz CH), 5.32–5.48 (m, 5H, 5 × CH), 4.39–4.43 (m, 1H, CH), 2.89–3.04 (m, 2H, CH_2), 2.77–2.86 (m, 2H, CH_2), 2.35–2.38 (m, 2H, CH_2), 2.10–2.15 (m, 2H, CH_2), 1.66–1.75 (m, 2H, CH_2), 1.46–1.53 (m, 2H, CH_2), 1.23–1.38 (m, 6H, 3 × CH_2), 0.85–0.88 (t, 3H, J = 6.85 Hz CH_3).

15-HpETE-G ^{1}H NMR at 500 MHz ($CDCl_3$): 6.58–6.63 (dd, 1H, J = 11.1, 15.3 Hz CH), 5.98–6.02 (t, 1H, J = 10.9 Hz CH), 5.56–5.61 (dd, 1H, J = 7.85, 15.3 Hz CH), 5.32–5.48 (m, 5H, 5 × CH), 4.38–4.42 (m, 1H, CH), 4.28–4.32 (t, 1H, J = 8.6 Hz CH), 4.09–4.26 (m, 1H, CH), 3.70–3.72 (m, 1H, CH), 3.60–3.63 (m, 1H, CH), 2.89–3.04 (m, 2H, CH_2), 2.77–2.86 (m, 2H, CH_2), 2.35–2.38 (m, 2H, CH_2), 2.10–2.15 (m, 2H, CH_2), 1.66–1.75 (m, 2H, CH_2), 1.46–1.53 (m, 2H, CH_2), 1.23–1.38 (m, 6H, 3 × CH_2), 0.85–0.88 (t, 3H, J = 6.85 Hz CH_3).

Detection of Endoperoxide Intermediates of PGHS Action—PGH_2, PGG_2, PGH_2-G, and PGG_2-G levels were determined from reactions of hPGHS-2 as follows. hPGHS-2 (400 nM) was reconstituted with an equivalent of hematin and incubated in 600 μl of 100 mM Tris-HCl, pH 8.0, with 500 μM phenol at 25 °C. Peroxide-free substrate was prepared and confirmed to be free of peroxides as described (16, 17). Substrate (AA or 2-AG) was added to a final concentration of 50 μM. Reactions were quenched with 600 μl of fresh anhydrous diethyl ether, vortexed for 10 s, and centrifuged at ~5000 rpm for 45 s. Ethereal fractions were removed and evaporated to dryness using a gentle stream of argon. Analytes were reconstituted in 300 μl of acetonitrile:water (50:50) and analyzed immediately. LC/MS was conducted on a Waters Acquity UPLC BEH C18 column (100 mm × 2.1 mm, 1.7 μm) using a gradient elution beginning with 100% A (5 mM NH_4OAc in H_2O, pH 3.3):0% B (5 mM NH_4OAc in 90% CH_3CN), and increasing linearly to 40% A:60% B over 7 min at 0.3 ml/min. Mass spectra were obtained on a ThermoFinnigan Quantum triple-quadrupole instrument equipped with an electrospray source and operated in positive ion mode with selected reaction monitoring. Quadrupoles 1 and 3 were set to the same mass for each analyte (ESI-MS *m/z* for PGH_2, 370.00 ($M+NH_4^+$); PGG_2, 386.00 ($M+NH_4^+$); PGH_2-G, 444.00 ($M+NH_4^+$); and PGG_2-G, 460.00 ($M+NH_4^+$).

O_2 Uptake Assay for the Cyclooxygenase Activity of PGHS—For determination of cyclooxygenase activity, pure PGHS protein (100–400 nM) was reconstituted with hematin and incubated in a 600-μl thermostatted cuvette, at 37 °C, in 100 mM Tris-HCl, pH 8.0, with 500 μM phenol. Peroxide-free substrate was added to a final concentration of 50 μM. Activity was monitored using an FO125T Instech fiber optic oxygen probe, connected to an Instech model 210 fiber optic oxygen monitor controlled with OOISensors software (Plymouth Meeting, PA). To test the effect of 15-HpETE and 15-HpETE-G in stimulating the turnover of 2-AG by H338Y mPGHS-2, either peroxide was added along with substrate to the final desired concentration.

Spectrophotometric Assay for Peroxidase Activity of PGHS—oPGHS-1, hPGHS-2, or mPGHS-2 (46 nM) was reconstituted with a half-equivalent of hematin in 80 mM Tris-HCl buffer, pH 8.0, containing 1 mM ABTS and incubated for 1 min. The mixture was added to a quartz cuvette and stirred continuously at 25 °C. 15-HpETE or 15-HpETE-G in acetonitrile was added to desired concentrations (78 nM–50 μM). The concentration of acetonitrile was maintained constant for all samples during a given experiment and never exceeded 5% of the total reaction volume (2 ml). The reaction was monitored via UV spectroscopy (417 nm) for the formation of the $ABTS^{+\cdot}$ radical. The early linear portions of the reaction curves were used to determine initial reaction rates at the various substrate concentrations (78 nM–50 μM). Plots of initial rates *versus* substrate concentration were fit to the Michaelis-Menten equation by nonlinear regression (Prism version 4.0).

GPx Activity—GPx activity was determined as described (18). Briefly, varying concentrations of 15-HpETE or 15-HpETE-G (78 nM–50 μM) were added to a mixture of 0.25 unit of GPx, 1 mM GSH, 1 unit of GSSG reductase, and 250 μM NADPH in 100 mM sodium phosphate buffer, pH 8.0, at 37 °C. The oxidation of NADPH was monitored via UV spectroscopy (340 nm). The early linear portions of the reaction curves were used to determine initial reaction rates, and the data were fit to the Michaelis-Menten equation via nonlinear regression. One unit of GPx catalyzes the oxidation by H_2O_2 of 1.0 μM GSH to oxidized GSH (GSSG) per min at pH 7.0 and 25 °C. One unit of GSSG reductase will reduce 1.0 μM GSSG per min at pH 7.6 at 25 °C.

Activation of Cyanide-inhibited oPGHS-1 and mPGHS-2 by 15-HpETE and 15-HpETE-G—Activation of PGHS enzymes by hydroperoxides was determined through the ability of the hydroperoxide to reduce the NaCN-induced lag phase in the cyclooxygenase reaction (19). The standard PGHS activity assay was modified to include 250 mM NaCN in the buffer. Peroxide-free AA along with varying concentrations of either 15-HpETE or 15-HpETE-G (15.6 nM–1 μM) was added to the cuvette. Activity was monitored as in the standard PGHS activity assay, with maximal rate determined by taking the first derivative of the reaction trajectory. Lag time (time to maximal rate) was determined for each concentration of peroxide (Prism version 4.0), for both oPGHS-1 and mPGHS-2, and plotted against the concentration of peroxide used. Statistical significance was determined using Student's *t* test (unpaired, two-tailed) using Prism (version 4.0) software.

GPx-mediated Suppression of AA and 2-AG Oxygenation by hPGHS-2 and mPGHS-2—The standard PGHS activity assay was modified to include 1 mM GSH and varying concentrations of GPx (20–160 units). Activity was monitored as above, with maximal rates achieved under each GPx concentration determined by taking the first derivative of the reaction trajectory. Maximal rates relative to the control (no GPx) were plotted against their respective concentration of GPx. Statistical significance was determined using Student's *t* test (unpaired, two-tailed) using Prism (version 4.0) software.

RNA Interference—Low passage murine NIH/3T3 fibroblasts were cultured in Dulbecco's modified Eagle's medium (DMEM) containing 10% heat-inactivated fetal bovine serum (FBS) and plated in 100-mm dishes at 75% confluence. Cells were cultured at 37 °C and 5% CO_2. shRNA plasmids (scrambled-negative control, GFP-positive control, Gpx4, and Gpx1) were obtained from Santa Cruz Biotechnology (Santa Cruz, CA). Transfection was carried out following the manufacturer's instructions, with selection of successfully transfected cells achieved by including 10 μg/ml puromycin (Sigma-Aldrich) in the growth medium. Selection was carried out for 2 weeks.

Immunoblotting for GPx Protein Expression—For the immunoblotting of GPx, monolayers of each shRNA-treated NIH/3T3 cell line from 35-mm dishes were lysed in 200 μl of M-PER lysis buffer (Thermo) containing a mixture of mammalian protease inhibitors (Sigma). Cell lysates were mixed on a Vortex Mixer and placed on ice for 30 min. Cellular debris was then removed by centrifugation for 10 min at 16,000 × *g*. Samples were stored at −80 °C until analyses could be completed. Equal quantities of protein (~ 20 μg) were resolved by gradient (2–12%) SDS-polyacrylamide gel electrophoresis and transferred onto a polyvinylidene difluoride membrane (Immobilon-P; Millipore). Membranes were blocked (20 mM Tris, pH 7.6, 140 mM NaCl, 0.05% Tween 20, 5% nonfat dry milk) prior to incubation with antibodies. The primary antibodies, mouse α-GPx1 (human/mouse/rat) and goat α-GPx4 (human/mouse/rat) (R&D Systems), were used at 1:1000 dilution and the secondary antibodies (α-mouse and α-goat) at 1:5000 (R&D Systems) dilution. Luminol-based detection was performed using SuperSignal West Pico reagents (Thermo Scientific).

Stimulation of PG and PG-G Synthesis in shRNA-treated Cell Lines—Murine NIH/3T3 fibroblasts were plated at 1×10^6 cells per well in 6-well dishes in DMEM containing 10 μg/ml puromycin and allowed to attach overnight. PG and PG-G production was stimulated by incubation with 12-*O*-tetradecanoylphorbol-13-acetate/ionomycin (0.08 μM/2 μM) for 4 h.

Assay for Production of PGs and PG-Gs by Cultured Cells—The medium from cell cultures was subjected to liquid-liquid extraction as described (20) with some modifications as follows. Briefly, internal standards ((100 pmol of the following: PGD_2-d_4, PGE_2-d_4, $PGF_{2\alpha}$-d_4, and 6-keto-$PGF_{1\alpha}$-d_4; and 10 pmol of the following: PGD_2-G-d_5, PGE_2-G-d_5, $PGF_{2\alpha}$-G-d_5, and 6-keto-$PGF_{1\alpha}$-G-d_5)) were added to medium (2 ml). The medium was acidified by the addition of glacial acetic acid to 1% (volume), followed by 2 ml of ethanol and 2 ml of hexanes:ethyl acetate (20:80 v:v). Samples were mixed and centrifuged at 3000 rpm for 20 min. The organic layer was retrieved and evaporated to dryness under a stream of nitrogen. Samples were resuspended in 300 μl of methanol:water (50:50 v:v) and analyzed as described previously (20).

Assay for Lipid Peroxidation and Oxidant Stress—shRNA-treated murine NIH/3T3 fibroblasts were cultured in DMEM with 10% FBS and plated in 100-mm dishes at 75% confluence. Cells were incubated with (2 μM) boron-dipyrromethene (BODIPY) 581/591 C11 (Invitrogen) overnight for flow cytometry analysis. When oxidized, BODIPY exhibits a shift in fluorescence from red to green (21). Cells were washed once with cold Ca^{2+}- and Mg^{2+}-free phosphate-buffered saline, trypsinized, and resuspended in 10% FBS DMEM. Cells (10,000) were loaded onto a 5-laser BD Biosciences LSRII flow cytometer, equipped with a 535-nm laser and analyzed with scrambled shRNA-treated NIH/3T3 as the base line for peroxidation. A histogram of the fluorescence of each group of cells in the range from red to green was generated, with a threshold set as P1 for cells exhibiting no shifts in fluorescence. The number of cells that demonstrated a shift in fluorescence from red to green for each cell line was tallied as a percentage of the entire population of the 10,000 cells. Analysis for the oxidative stress marker, 8-isoprostane (8-epi $PGF_{2\alpha}$) was carried out as published previously (22).

TABLE 1
Steady-state kinetic parameters for PGHS-1 and PGHS-2 mediated oxidation of ABTS by 15-HpETE and 15-HpETE-G
The data represent mean ± S.E. of quadruplicate determinations.

15-HpETE or 15-HpETE-G	K_m	k_{cat}	k_{cat}/K_m
	μM	s^{-1}	$s^{-1} \cdot$ μM
15-HpETE			
oPGHS-1	4.9 ± 1.3	34.0 ± 3.0	6.9 ± 2.3 NS[a]
mPGHS-2	1.0 ± 0.2	6.6 ± 0.3	6.4 ± 1.5[b]
hPGHS-2	3.0 ± 0.5	9.3 ± 0.4	3.2 ± 0.8 NS
15-HpETE-G			
oPGHS-1	4.5 ± 1.2	49.0 ± 4.0	11.0 ± 3.3 NS
mPGHS-2	8.0 ± 2.0	15.0 ± 1.0	1.9 ± 0.5[b]
hPGHS-2	4.8 ± 0.5	16.1 ± 0.4	3.4 ± 0.8 NS

[a] NS, not significant.
[b] Student's *t* test, unpaired, two-tailed, comparing the k_{cat}/K_m values for 15-HpETE and 15-HpETE-G for the same enzyme, $p < 0.001$.

RESULTS

Glyceryl Hydroperoxides as Substrates for the Peroxidase Activities of mPGHS-2, hPGHS-2, and oPGHS-1—To determine whether the glyceryl ester affects the efficiency of the PGHS peroxidase, we determined the steady-state kinetic values for the reduction of 15-HpETE and 15-HpETE-G. 15-HpETE is comparable with PGG_2 as a peroxidase substrate and has been used as a model for PGG_2, which is unstable and difficult to prepare in highly purified form (23, 24). By extension, we used 15-HpETE-G as a surrogate for PGG_2-G. Both hydroperoxides were prepared and tested as described under "Experimental Procedures." Heme-reconstituted mPGHS-2, hPGHS-2, or oPGHS1 was incubated with increasing concentrations of 15-HpETE or 15-HpETE-G and 1 mM reducing substrate ABTS. Table 1 summarizes the k_{cat} and K_m values for the two substrates and the three enzymes. 15-HPETE and 15-HPETE-G are comparable substrates for all three enzymes. In the case of hPGHS-2 and oPGHS-1, the k_{cat}/K_m values for the two substrates were not significantly different. For mPGHS-2, the k_{cat}/K_m was 3-fold higher for 15-HPETE than for 15-HPETE-G, a difference that reached statistical significance. This was mainly because of a much higher K_m for 15-HPETE-G. Thus, 15-HpETE and 15-HpETE-G are comparable substrates for the peroxidase activities of oPGHS-1 and hPGHS-2. This suggests that there are not dramatic differences in the rates of reduction of hydroperoxy derivatives of AA and 2-AG by the peroxidase activities of either PGHS-1 or PGHS-2.

We were unable to prepare PGG_2-G for studies of its reduction by the PGHS-2 peroxidase, so we developed an LC/MS-based method to monitor the flux of endoperoxide intermedi-

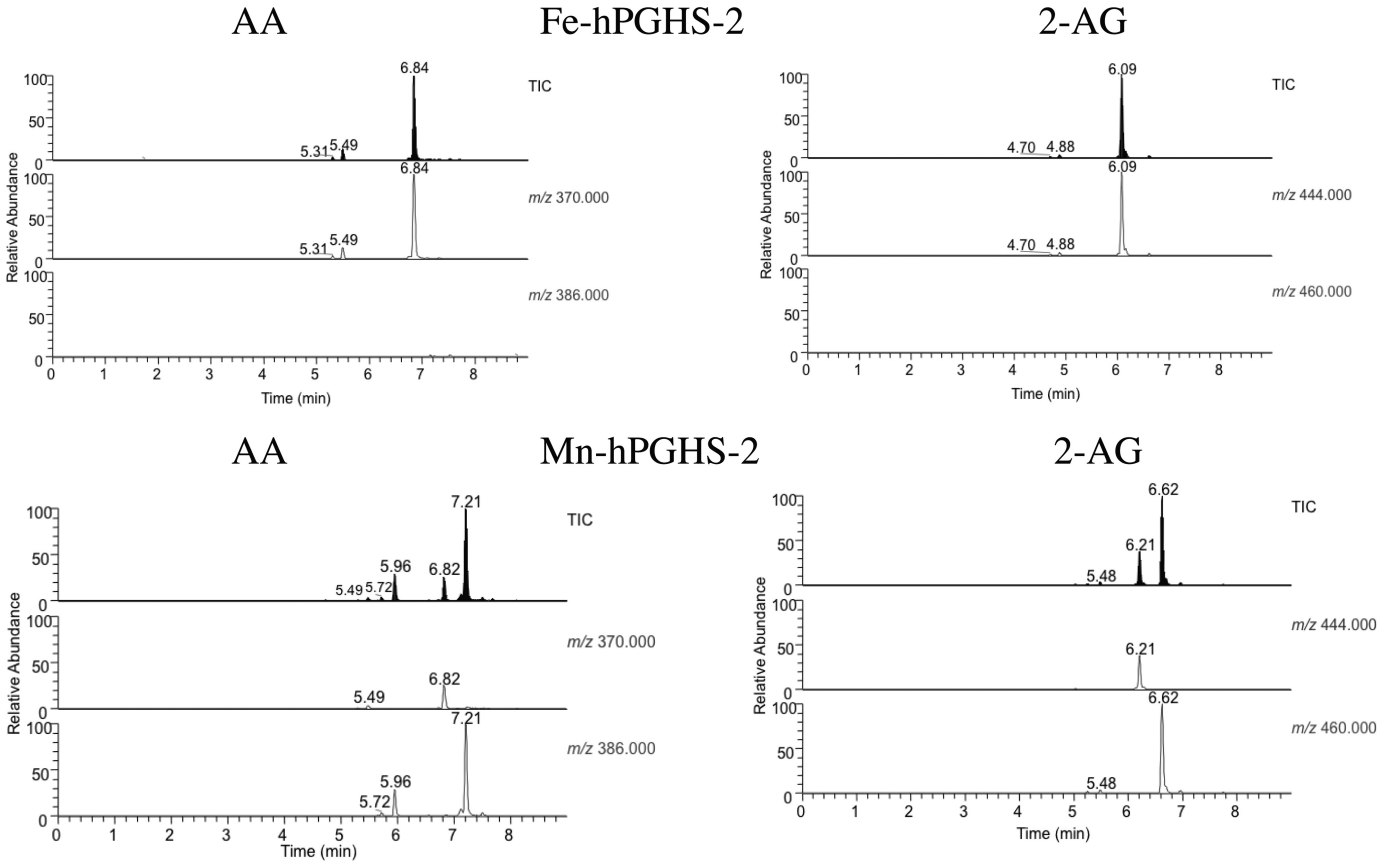

FIGURE 2. **Products of oxygenation of AA and 2-AG by Fe-hPGHS-2 and Mn-hPGHS-2.** AA or 2-AG was incubated with Fe- or Mn-reconstituted PGHS-2 for 30 s and the products extracted and analyzed by LC/MS as described under "Experimental Procedures." PGH_2 and PGH_2-G elute at 6.84 and 6.09 min, respectively, whereas PGG_2 and PGG_2-G elute at 7.21 and 6.62. The minor peaks eluting at 5.7 and 5.9 min are PGs. No residual AA or 2-AG was detected.

ates during PGHS-2 catalysis. We incubated hPGHS-2 with AA or 2-AG for 30 s, extracted the incubation mixtures with cold diethyl ether, and analyzed the extracts by LC/MS. Fig. 2 compares the total ion chromatograms and selected ion monitoring profiles of extracts of AA and 2-AG incubated with Fe-hPGHS-2 or Mn-hPGHS-2. With Fe-hPGHS-2 and AA, a major peak was observed at 6.8 min with *m*/*z* 370, corresponding to PGH_2, and with Fe-hPGHS-2 and 2-AG, a major peak was observed at 6.1 min with *m*/*z* 444 corresponding to PGH_2-G. No peaks were observed in either incubation with *m*/*z* 386 or *m*/*z* 460, corresponding to PGG_2 or PGG_2-G, respectively. Thus, AA and 2-AG are oxygenated to PGG_2 and PGG_2-G, respectively, and both endoperoxides are efficiently reduced to PGH_2 and PGH_2-G.

Parallel experiments were performed with Mn-PGHS-2, which exhibits peroxidase activity >200-fold lower than Fe-PGHS-2 but retains full cyclooxygenase activity (25). Incubations of AA and Mn-hPGHS-2 generated LC/MS profiles exhibiting a major peak at 7.2 min with *m*/*z* 386 that coeluted with a commercial sample of PGG_2. A small peak of PGH_2 was detected at 6.8 min, and minor peaks at 5.4–5.9 min corresponded to hydroperoxy-PGs. Incubations of 2-AG and Mn-hPGHS-2 generated LC/MS profiles exhibiting a major peak at 6.6 min with an *m*/*z* 460 corresponding to PGG_2-G. A small peak of PGH_2-G was observed at 6.2 min, and a trace peak at 5.4 min corresponded to hydroperoxy-PG-Gs. These experiments, although qualitative, indicate that PGG_2-G and PGH_2-G are detectable in incubations of 2-AG with hPGHS-2 and that PGG_2-G is efficiently reduced to PGH_2-G by the peroxidase activity of hPGHS-2. The results support the conclusions summarized in Table 1 that the glyceryl esters of 15-HPETE and PGG_2 are comparable with the free acids as substrates for the peroxidase activity of PGHS-2.

Activation of the Oxygenase Activity in oPGHS-1 and mPGHS-2 by 15-HpETE and 15-HpETE-G—After establishing the steady-state kinetics for the reduction of 15-HpETE and 15-HpETE-G by the peroxidase activities of oPGHS-1, hPGHS-2, and mPGHS-2, we evaluated the ability of 15-HpETE and 15-HpETE-G to activate oPGHS-1- and mPGHS-2-mediated oxygenation of AA in the presence of NaCN, as described under "Experimental Procedures." High concentrations of CN^- bind to the active site heme of PGHS and inhibit cyclooxygenase activation, leading to a lag phase in reaction progress curves. This can be overcome by addition of hydroperoxide activators. The time taken to achieve maximal rate was plotted against the concentration of exogenous peroxide added (Fig. 3). 15-HpETE and 15-HpETE-G demonstrated a concentration-dependent diminution in the time taken to achieve maximal turnover of AA with both oPGHS-1 (Fig. 3*A*) and mPGHS-2 (Fig. 3*B*). These results are consistent with the peroxidase kinetics for oPGHS-1, where 15-HpETE and 15-HpETE-G did not differ in efficiency as peroxidase substrates. Likewise, there was no statistically significant difference in the ability of 15-HpETE and 15-HpETE-G to activate

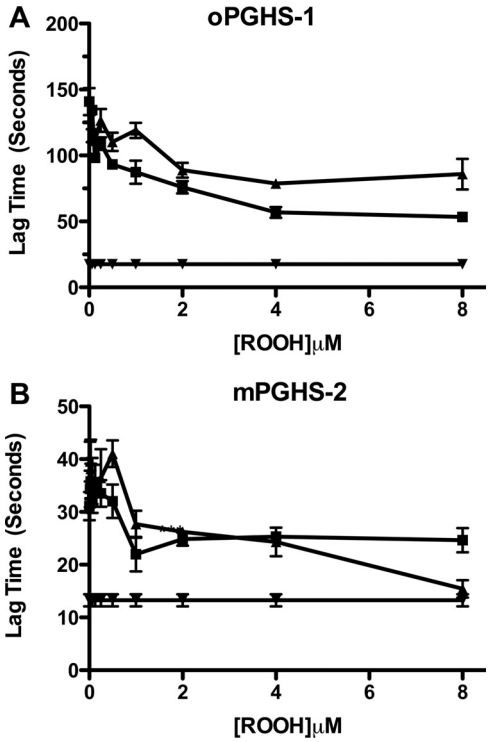

FIGURE 3. **Activation of oxygenase activity in oPGHS-1 (*A*) and mPGHS-2 (*B*) by 15-HpETE and 15-HpETE-G.** A lag was induced in the turnover of AA by incubating either oPGHS-1 (60 nM, *A*) or mPGHS-2 (120 nM, *B*) in standard assay buffer containing 250 mM NaCN. Lag time was defined as the time to maximal rate of oxygen consumption. Lag time was plotted against the final concentration of either 15-HpETE (■) or 15-HpETE-G (▲) in the cuvette. The lag time in the absence of 250 mM NaCN and exogenous peroxide (▼) was also plotted. The data are from triplicate determinations and are reported as mean ± S.E. (*error bars*). The differences between the curves were not statistically significant.

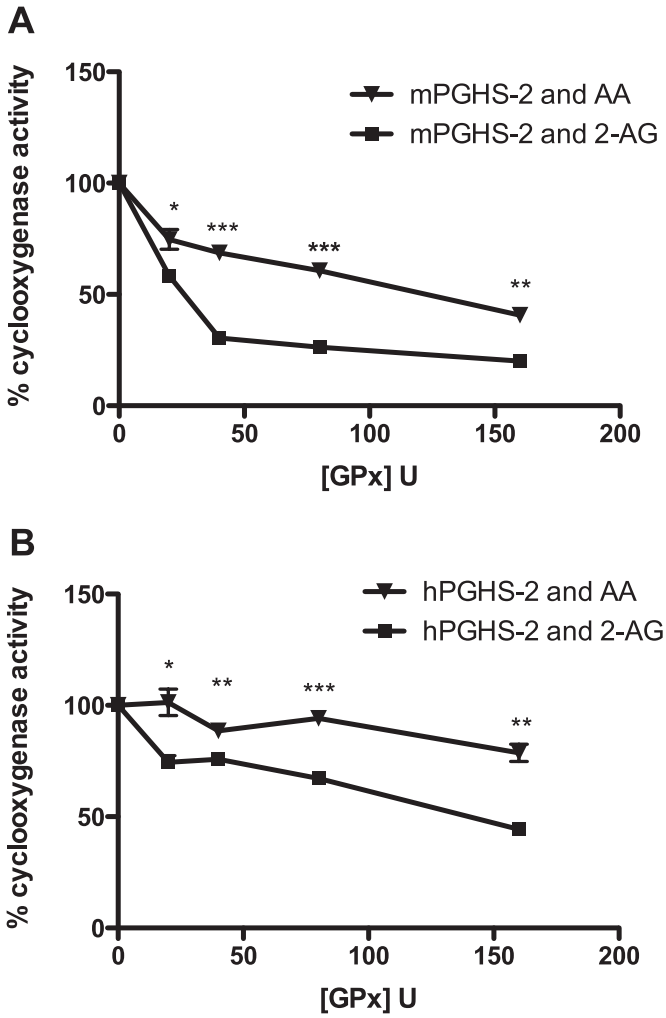

FIGURE 4. **Suppression of the oxygenation of AA and 2-AG by GPx-GSH.** mPGHS-2 (400 nM, *A*) or hPGHS-2 (400 nM, *B*) was incubated with increasing concentrations of GPx (0–160 units) in standard assay buffer, and AA (▼) or 2-AG (■) was added to 50 μM as described under "Experimental Procedures." The maximal rate of oxygen consumption relative to the control (no GPx) was plotted against the concentration of GPx. Data are from triplicate determinations. *Asterisks* indicate statistically significant differences in the relative rate of oxygen consumption between AA and 2-AG (Student's *t* test, unpaired, two-tailed; *, $p < 0.05$; **, $p < 0.001$; ***, $p < 0.0001$).

mPGHS-2, despite the difference observed in the steady-state kinetics for reduction of 15-HpETE *versus* 15-HpETE-G (Table 1). Therefore, AA- and 2-AG-derived hydroperoxides are equivalent activators of cyclooxygenase activity for both PGHS-1 and PGHS-2.

Reduction of 15-HpETE and 15-HpETE-G by GPx—Addition of high concentrations of GSH and GPx inhibits cyclooxygenase activation by scavenging fatty acid hydroperoxides before they can react with the PGHS active site heme. Prior to evaluating the impact of GSH/GPx on cyclooxygenase activity, we compared the ability of GSH/GPx to reduce 15-HPETE and 15-HPETE-G, as described under "Experimental Procedures" (data not shown). 15-HpETE appeared to be a better substrate for GPx as judged by the extent of GSH oxidation, but kinetic parameters could not be determined because of the limit of the solubility of the substrates. In fact, the critical micelle concentration for 15-HpETE-G is ~70 μM (data not shown). Thus, it appears as though AA-derived hydroperoxide is a better substrate for GPx than 2-AG-derived hydroperoxide.

GPx-mediated Suppression of the Oxygenation of AA and 2-AG by mPGHS-2 and hPGHS-2—When mPGHS-2 or hPGHS-2 was incubated with increasing concentrations of GPx in the presence of 1 mM GSH, the relative reduction in the rate of oxygenation of 2-AG was significantly greater than the reduction in the rate of oxygenation of AA (Fig. 4). The decrease in oxygenase activity was dependent on the

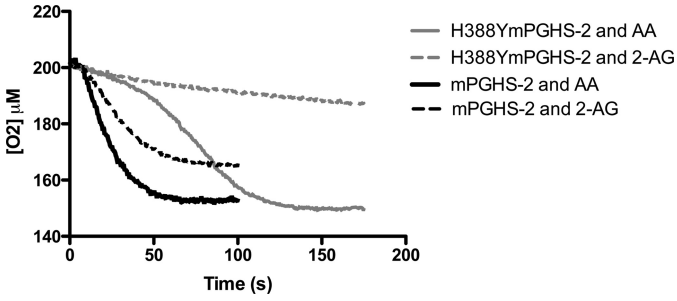

FIGURE 5. **Oxygenation of AA and 2-AG by H388Y mPGHS-2.** 400 nM WT mPGHS2 was incubated with a 50 μM concentration of either AA (*solid line*) or 2-AG (*broken line*), in standard assay buffer, as described under "Experimental Procedures." For comparison, H388Y mPGHS2 was incubated with a 50 μM concentration of either AA (*solid line*) or 2-AG (*broken line*), in standard assay buffer as described under "Experimental Procedures." *Traces* are representative of triplicate determinations. In a single experiment, the end point values for each curve varied by no more than 5%.

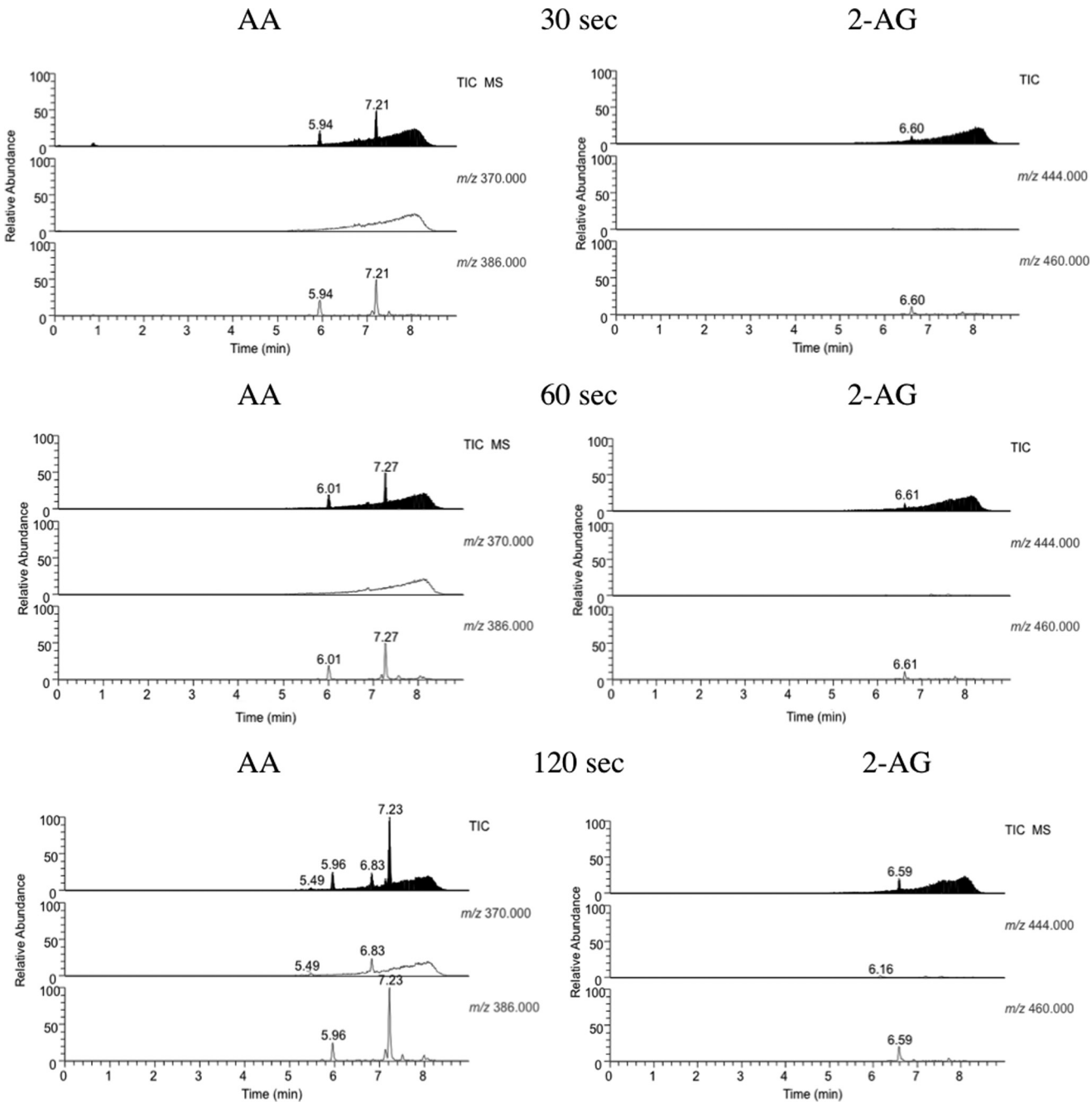

FIGURE 6. **Comparison of the production of PGG_2 and PGG_2-G on incubation of AA and 2-AG with H388Y mPGHS-2.** The levels of PGG_2 and PGG_2-G produced by the oxygenation of AA and 2-AG over the course of oxygenation by H388Y mPGHS-2 were determined as described under "Experimental Procedures." PGG_2 eluted at 7.21 min and PGG_2-G at 6.61 min. PGH_2 eluted at 5.9–6.1 min.

concentration of GPx incubated with either mPGHS-2 or hPGHS-2 (Fig. 4). These experiments show that the oxygenation of 2-AG, relative to AA, demonstrates greater sensitivity to suppression by GPx.

Oxygenation of 2-AG by Purified Recombinant H388Y mPGHS-2—Because the oxygenation of 2-AG appears more sensitive to peroxide tone than the oxygenation of AA, we investigated 2-AG oxygenation by an mPGHS-2 mutant (H388Y) that has greatly diminished peroxidase activity (12). Fig. 5 displays the oxygenation of AA and 2-AG by purified recombinant mPGHS-2 and purified recombinant H388Y mPGHS-2. The turnover of AA by H338Y mPGHS-2 displays a characteristic lag in its initial trajectory relative to the wild-type mPGHS-2 (Fig. 5), reflective of the diminished peroxidase activity of the mutant enzyme which results in reduced activation of cyclooxygenase activity (12). Despite this lag, the final extent of oxygenation of AA by H388Y mPGHS-2 was the same as that by wild-type mPGHS-2, once full activation was achieved. In contrast, the turnover of 2-AG by H388Y was severely diminished relative to the turnover of 2-AG by wild-type mPGHS-2 (Fig. 5). Neither a clear-cut lag phase nor an accelerative phase in oxygenation was observed. This result, along with the finding that 2-AG turnover was more sensitive to GPx suppression, indicated that 2-AG oxygenation is more sensitive to peroxide activation than AA oxygenation.

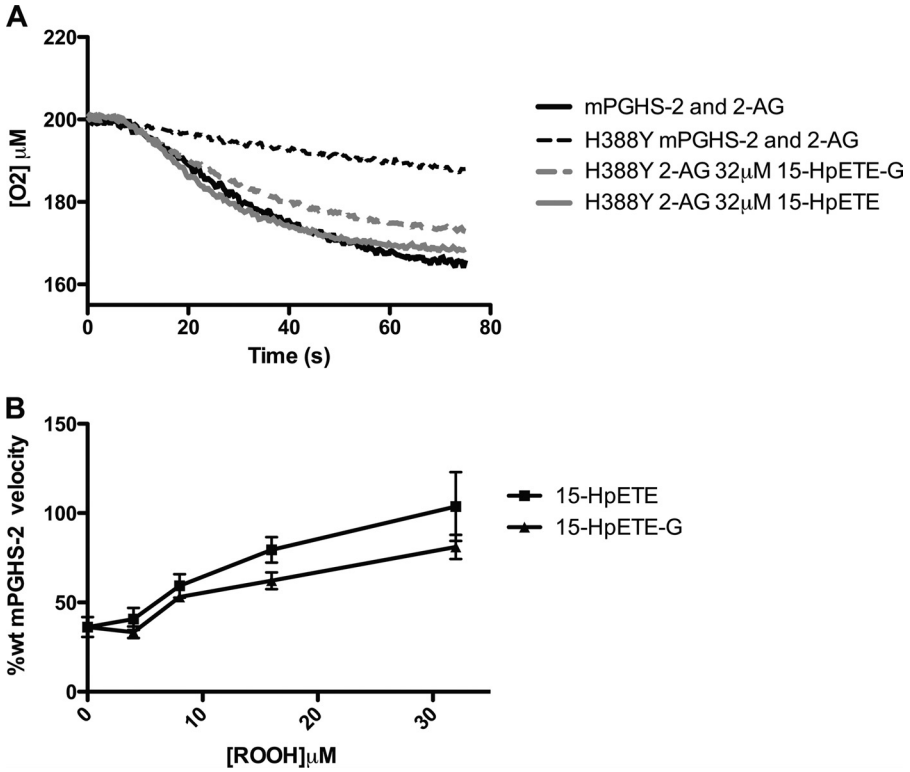

FIGURE 7. **Stimulation of oxygenation of 2-AG by H388Y mPGHS-2 by 15-HpETE and 15-HpETE-G.** 400 nM WT mPGHS2 was incubated with 50 μM 2-AG (*solid lines*), in standard assay buffer, as described under "Experimental Procedures." *A*, for comparison, H388Y mPGHS-2 was incubated with 50 μM 2-AG alone (*broken lines*), or with either 32 μM 15-HpETE (*solid line*) or 32 μM 15-HpETE-G (*broken line*) in standard assay buffer as described under "Experimental Procedures." *B*, a plot of the rate of H388Y mPGHS-2-mediated 2-AG turnover, relative to that of wild-type mPGHS-2, was generated over a range of concentrations (4-32 μM) of either 15-HpETE (■) or 15-HpETE-G (▲). Data are from triplicate determinations and are reported as mean ± S.E. (*error bars*). The differences between 15-HpETE and 15-HpETE-G were not statistically significant.

These results were supported by endoperoxide profiling of H388Y catalysis (Fig. 6). In incubations of AA and H388Y, a peak at 7.2 min with *m*/*z* 386 corresponding to PGG_2 was observed and increased at longer times. No peak was observed for PGH_2 with *m*/*z* 370, which is consistent with the dramatically reduced peroxidase activity of the H388Y mutant. In contrast, the peak at 6.6 min with *m/z* 460, which corresponds to PGG_2-G, was present in very low abundance and scarcely increased with longer incubation times. This indicates that PGG_2-G levels never approached those of PGG_2. Thus, the peroxide tone necessary to initiate the accelerative phase of the cyclooxygenase reaction could not be achieved when 2-AG was the substrate.

Stimulation of 2-AG Oxygenation by Purified Recombinant H388Y mPGHS-2 via 15-HpETE and 15-HpETE-G—The severe impairment in the oxygenation of 2-AG by H388Y mPGHS-2 could be due to reduced peroxidase activation of cyclooxygenase activity or to differences in substrate-enzyme interaction. To test the role of reduced peroxidase activation, we incubated H388Y mPGHS-2 with increasing concentrations of either 15-HpETE or 15-HpETE-G. Fig. 7*A* demonstrates that incubation with either 32 μM 15-HpETE or 32 μM 15-HpETE-G led to increases in the rate and extent of 2-AG oxygenation to those observed with wild-type enzyme. The recovery of 2-AG oxygenation by H388Y mPGHS-2 was dependent on the concentration of 15-HpETE and 15-HpETE-G, with both demonstrating comparable capacity to overcome the lack of 2-AG turnover (Fig. 7*B*).). Although other factors may be at play in the diminished turnover of 2-AG by H388Y mPGHS-2, these data indicate that a major determinant of the diminished turnover of 2-AG by H388Y mPGHS-2 is due to a constant requirement for peroxide for 2-AG turnover. Furthermore, these data provide further verification that exogenously provided 15-HpETE and 15-HpETE-G are equivalent activators of cyclooxygenase activity.

Effect of shRNA Silencing of GPx4 and GPx1 on Cellular PG and PG-G Synthesis—To probe the effect of peroxide tone on cellular PGHS-2 action, we silenced the phospholipid hydroperoxide-specific GPx4, which may play a role in regulating hydroperoxide levels in membrane compartments. In parallel, GPx1, which is the major cytosolic GPx, was silenced. shRNA-mediated GPx depletion was determined by immunoblotting for each respective GPx. Relative to the scrambled control, a knockdown of ~75% of GPx4 and ~50% of GPx1 was achieved (Fig. 8).

Determination of the Effect of GPx4 and GPx1 Knockdown on Peroxide Tone and Oxidant Stress—Following the determination that substantial depletion of GPx4 and GPx1 was achieved, we evaluated the levels of lipid peroxidation in each cell line as described under "Experimental Procedures." Flow cytometric analysis of BODIPY-treated cells revealed a 3-fold higher level of lipid peroxidation in anti-GPx4 shRNA-treated fibroblasts relative to scrambled control shRNA-treated fibroblasts (Fig. 9). Interestingly, examination of the histograms from the BODIPY assay indicates that the anti-GPx4 shRNA-treated fibroblasts display a bimodal distribution in the population.

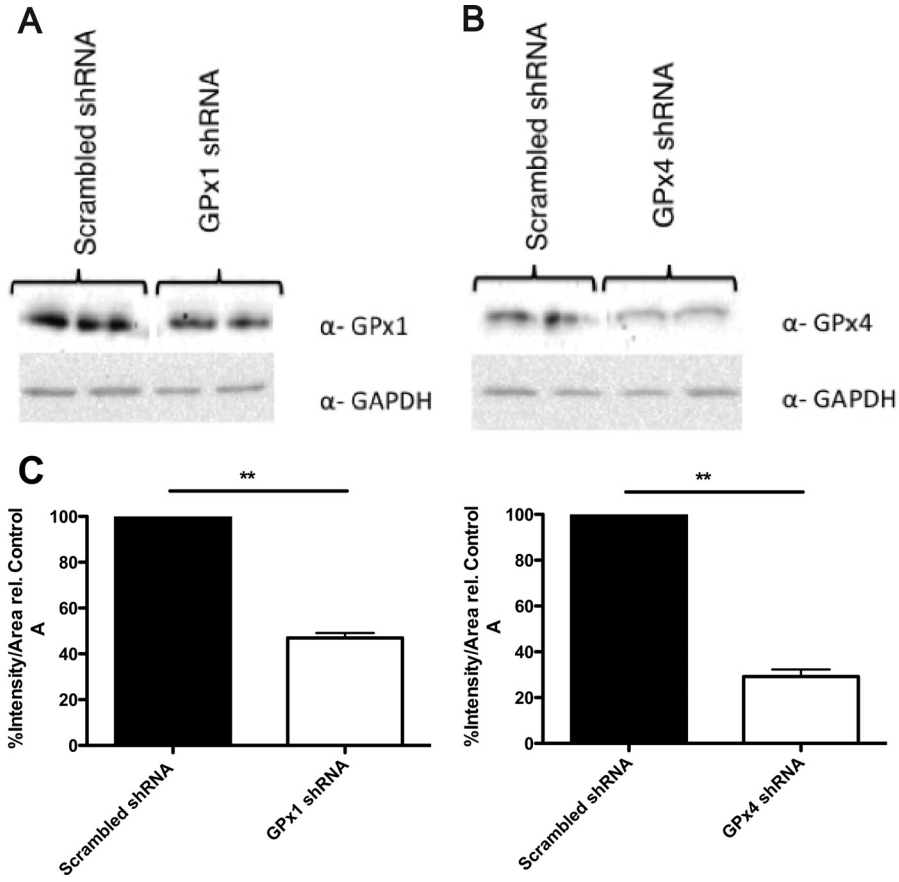

FIGURE 8. **Determination of the levels of GPx1 and GPx4 following shRNA-mediated silencing.** *A* and *B*, immunoblots for GPx1 and GPx4 in NIH/3T3 fibroblasts transfected with shRNA plasmids to silence GPx1 and GPx4 as described under "Experimental Procedures." *C*, densitometry quantification of results from the immunoblots. *Asterisks* indicate statistically significant differences in the levels of GPx1 and GPx4 in GPx1 and GPx4 shRNA-transfected NIH/3T3 fibroblasts, relative to the scrambled shRNA (negative control) (Student's *t* test, unpaired, two-tailed, **, $p < 0.001$). Values are reported as mean ± range of duplicate determinations.

Part of this population extends past the threshold of transition from red to green fluorescence, P1, indicating that a significant proportion of these cells is exhibiting a shift in fluorescence away from base line, indicative of increased BODIPY oxidation (21). This is in comparison with scrambled control and anti-GPx1 shRNA-treated fibroblasts. Furthermore, measurement of levels of the oxidant stress biomarker, 8-isoprostane, revealed that anti-GPx4 shRNA-treated fibroblasts demonstrate statistically significantly higher levels of this marker relative to scrambled control and anti-GPx1 shRNA-treated fibroblasts (Fig. 10). The similarity in the extent of oxidant stress in anti-GPx1 shRNA-treated fibroblasts and scrambled shRNA-treated cells suggests that GPx1 is not involved in protecting cells against lipid peroxidation or that the activity of GPx1 was not sufficiently decreased at this level of knockdown to observe an effect on oxidant stress parameters.

Determination of the Effect of GPx4 and GPx1 Knockdown on PG and PG-G Synthesis—Following the demonstration that depletion of GPx4 could lead to increased lipid peroxidation, we determined the effect of increased peroxide tone on PG and PG-G synthesis. Addition of 12-*O*-tetradecanoylphorbol-13-acetate and ionomycin stimulated the production of PG and PG-Gs from endogenous sources. Scrambled control, anti-GPx1, and anti-GPx4 shRNA-treated fibroblasts all demonstrated similar levels of PG synthesis (Fig. 10). In contrast, the two major species of PG-Gs generated by fibroblasts, PGE_2-G and $PGF_{2\alpha}$-G, were elevated 2- and 4-fold, respectively, in anti-GPx4 shRNA-treated fibroblasts, relative to the scrambled control shRNA-treated fibroblasts. Anti-GPx1 shRNA-treated fibroblasts, which did not show increases in oxidative stress parameters, did not differ from scrambled shRNA-treated cells with regard to PG-G synthesis.

DISCUSSION

The present study compared the ability of hydroperoxide derivatives of AA and 2-AG to serve as substrates for the peroxidase activities of PGHS-1 and PGHS-2 and as activators of the cyclooxygenase activities of both enzymes. The results clearly show that the 15-hydroperoxy derivatives of both molecules are similar in their efficiencies as substrates for the PGHS-1 and PGHS-2 peroxidases, and that, when added exogenously, they activate the cyclooxygenase activities of the two enzymes equivalently with AA as the substrate (Table 1 and Fig. 7). The k_{cat}/K_m values for oxidation of ABTS by the peroxidase activity of PGHS-1 and PGHS-2 are similar for 15-HPETE and 15-HPETE-G, although there are some differences (Table 1). oPGHS-1 exhibits a k_{cat}/K_m for 15-HPETE-G that is not statistically significantly higher than that for 15-HPETE, whereas mPGHS-2 exhibits a k_{cat}/K_m for 15-HPETE that is nearly 3-fold higher than for 15-HPETE-G. Ultimately, these differences in steady-state kinet-

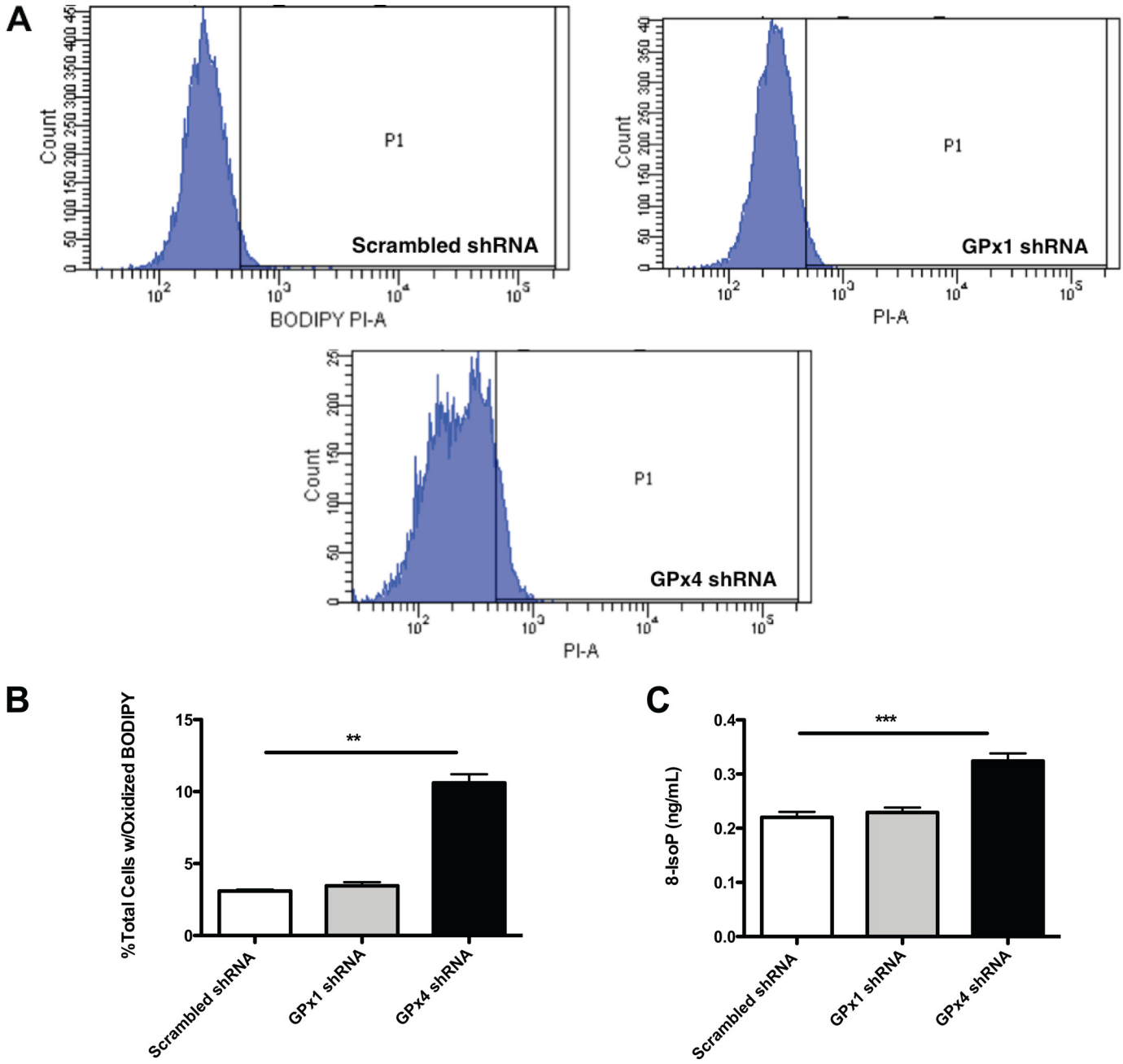

FIGURE 9. **Effect of shRNA-mediated silencing of the GPx system on peroxide tone in murine NIH/3T3 fibroblasts.** Lipid peroxidation was assayed using the membrane-specific dye BODIPY and flow cytometry as described under "Experimental Procedures." *A*, histograms of 10,000 cell counts for each shRNA-treated cell line. A larger proportion of anti-GPx4 shRNA-transfected 3T3 fibroblasts demonstrates a green fluorescence shift from red as BODIPY is oxidized past the threshold P1 (**, $p < 0.001$). *B*, quantitation of the proportions of cells shifting fluorescence past the threshold (P1) (**, $p < 0.001$). S.E. *C*, assay of the oxidative stress marker, 8-IsoP, in the control, anti-GPx1- and anti-GPx4-transfected fibroblasts (Student's *t* test, unpaired, two-tailed. ***, $p < 0.0001$). Values are reported as mean ± S.E. (*error bars*).

ics did not correlate with any differences in activation of the respective enzyme cyclooxygenase activities (Figs. 3 and 7).

Although hydroperoxy derivatives of 2-AG and AA are equivalent in their ability to activate PGHS-1 and PGHS-2, we discovered significant differences between the sensitivity of oxygenation of 2-AG and AA to conditions of limiting peroxidase-dependent activation. This was unanticipated because 2-AG and AA have similar k_{cat}/K_m values for oxidation by human or mouse PGHS-2 (10). However, reduction of peroxidase-dependent cyclooxygenase activation by hydroperoxide scavenging with GSH and GPx or utilization of an mPGHS-2 mutant (H388Y) with significantly reduced peroxidase activity disproportionately affects 2-AG oxygenation compared with that of AA. This is especially dramatic in experiments with the H388Y mutant (Fig. 5). As reported previously, oxygenation of AA by this mutant occurs with a pronounced lag phase, but eventually an accelerative phase of oxygenation occurs, and the extent of reaction equals that observed with AA by wild-type PGHS-2 (12). In contrast, the lag phase for oxygenation of 2-AG by H388Y is so pronounced that an accelerative phase is not observed, and the enzyme never attains a robust rate of 2-AG oxygenation (Fig. 7).

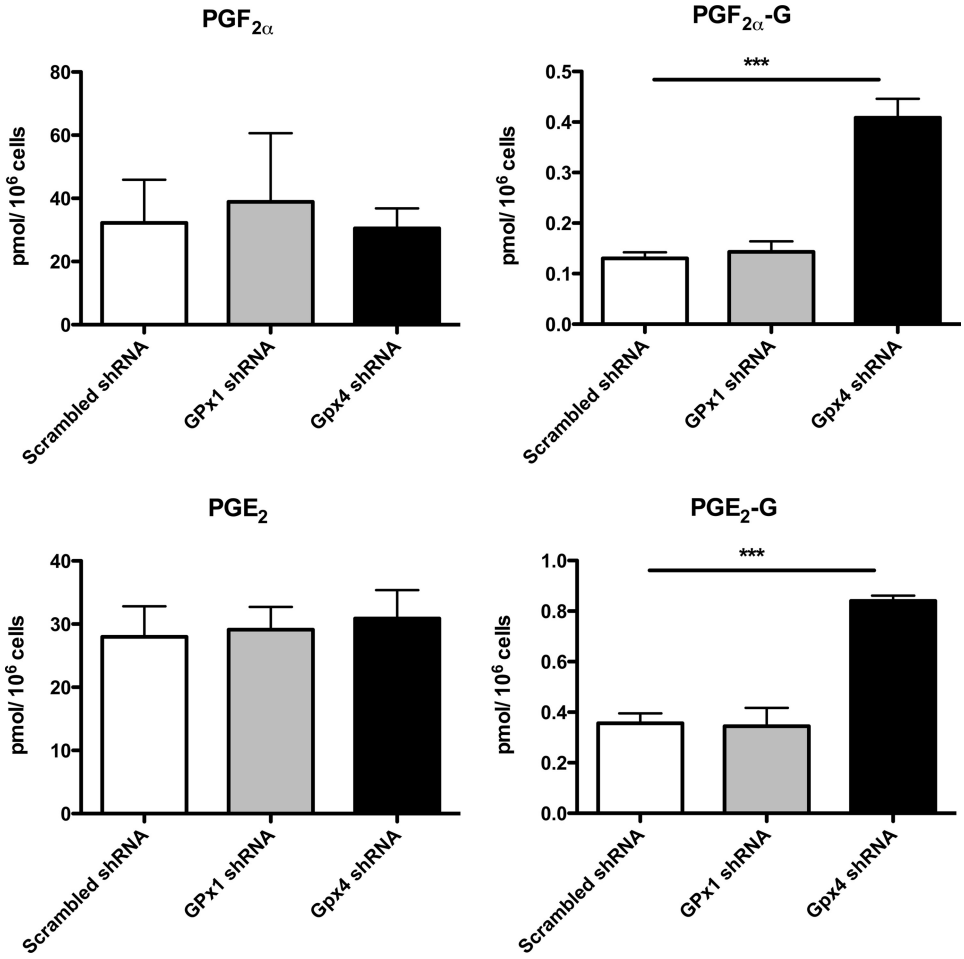

FIGUR E 10. **Impact of shRNA-mediated silencing of the GPx system on PG and PG-G production by murine 3T3 fibroblasts.** shRNA-transfected 3T3 fibroblasts were stimulated as described under "Experimental Procedures," and culture medium was analyzed as described for PG and PG-G production. *Asterisks* indicate statistically significant differences in the levels of PG-Gs measured from GPx4 and scrambled shRNA-transfected NIH/3T3 fibroblasts, relative to the scrambled shRNA (negative control) NIH/3T3 fibroblasts (Student's *t* test, unpaired, two-tailed, ***, $p < 0.0001$). Values are reported as mean ± S.E. (*error bars*).

The inability of H388Y to oxygenate 2-AG, which is due to a rate of hydroperoxide generation from 2-AG insufficient to rapidly activate other inactive PGHS-2 molecules (Fig. 6), is overcome by the addition of hydroperoxide (Fig. 7). This suggests the reduced peroxidase-dependent cyclooxygenase activation by H388Y is the major determinant of reduced 2-AG oxygenation by this mutant. Although the k_{cat}/K_m values of AA and 2-AG oxygenation by wild-type PGHS-2 are similar, there are differences in their oxygenation that are only unmasked under conditions of peroxidase deficiency. This inherent difference in the requirement for sustained activation of oxygenation with 2-AG relative to AA explains why 2-AG oxygenation demonstrates sensitivity to decreased peroxide tone. Other factors may also contribute to the diminished oxygenation of 2-AG by H388Y, but the ability of hydroperoxides to restore wild-type levels of oxygenation suggests that the major factor is diminished hydroperoxide-dependent cyclooxygenase activation.

The increased sensitivity of 2-AG relative to AA to reduced peroxide tone is reminiscent of the behavior of eicosapentaenoic acid with PGHS-1. Eicosapentaenoic acid is a poor substrate for oxygenation by PGHS-1, but its oxidation is stimulated by exogenous peroxide (26). Examination of the crystal structure of eicosapentaenoic acid with PGHS-1 demonstrates a shift in the conformation of Tyr-385 from its critical position near the 13-*pro-S*-hydrogen, leading to poor initiation of eicosapentaenoic acid oxygenation relative to AA (27). Recent crystallographic studies of 1-AG bound to Co^{3+}-murine PGHS-2 reveal that the endocannabinoid binds in a productive conformation in one subunit and a nonproductive conformation in the other subunit of the homodimer. The differences between the productive and nonproductive conformations involve the extent to which the ω-end of the substrate inserts into the hydrophobic channel above Ser-530 (28). There also appear to be slight differences in the productive conformations of 1-AG and AA bound to Co^{3+}-PGHS-2 with regard to the alignment of the 13-*pro-S*-hydrogens of the two substrates with Tyr-385 (28). These subtle conformational differences may make the individual steps in oxygenation of endocannabinoid substrates less efficient than the same steps in the oxygenation of AA. For example, suboptimal alignment of Tyr-385 or the Tyr-385 tyrosyl radical with either 2-AG/1-AG or transient intermediates in PGG_2-G generation could slow the rate of the individual steps in oxygenation such as the regeneration of the catalytically active tyrosyl radical at the end of oxygenation. Release of a PGG_2-G peroxyl radical before oxidation of Tyr-385 would

result in inactive enzyme that would need to be activated by another molecule of hydroperoxide. This would explain the increased need for peroxide in the oxygenation of 2-AG relative to AA, reflecting a continued need to regenerate the Tyr-385 radical by the peroxidase activity.

Statistically significant increases in lipid peroxidation and oxidative stress were observed in anti-GPx4 shRNA-transfected murine 3T3 fibroblasts. This was associated with up to a 4-fold increase in PG-G production over both scrambled shRNA and anti-GPx1 shRNA-transfected fibroblasts. These cellular data are in line with previous demonstrations that increased peroxide scavenging by the endogenous peroxide detoxification mechanism (the GPx family) can lead to decreased prostanoid production, directly due to decreased peroxide tone and oxidant stress (29). Here we extend that finding to the endocannabinoid, 2-AG, and propose that under states of inflammation, where oxidant stress is high, oxygenation of 2-AG by PGHS-2 may be augmented. This increased endocannabinoid oxygenation may be an important contributor to a pain response due to increased degradation of the analgesic 2-AG and the generation of hyperalgesic and allodynic PG-Gs such as PGE_2-G (9).

Acknowledgments—We are grateful to Carol Rouzer for the careful reading of this manuscript and Phillip Kingsley and Ginger Milne for technical assistance with eicosanoid analysis.

REFERENCES

1. Van der Ouderaa, F. J., Buytenhek, M., Nugteren, D. H., and Van Dorp, D. A. (1977) Purification and characterization of prostaglandin endoperoxide synthetase from sheep vesicular glands. *Biochim. Biophys. Acta* **487,** 315–331
2. Rouzer, C. A., and Marnett, L. J. (2003) Mechanism of free radical oxygenation of polyunsaturated fatty acids by cyclooxygenases. *Chem. Rev.* **103,** 2239–2304
3. Kulmacz, R. J., and Wang, L. H. (1995) Comparison of hydroperoxide initiator requirements for the cyclooxygenase activities of prostaglandin H synthase-1 and -2. *J. Biol. Chem.* **270,** 24019–24023
4. Rouzer, C. A., and Marnett, L. J. (2008) Nonredundant functions of cyclooxygenases: oxygenation of endocannabinoids. *J. Biol. Chem.* **283,** 8065–8069
5. Devane, W. A., Hanus, L., Breuer, A., Pertwee, R. G., Stevenson, L. A., Griffin, G., Gibson, D., Mandelbaum, A., Etinger, A., and Mechoulam, R. (1992) Isolation and structure of a brain constituent that binds to the cannabinoid receptor. *Science* **258,** 1946–1949
6. Stella, N., Schweitzer, P., and Piomelli, D. (1997) A second endogenous cannabinoid that modulates long-term potentiation. *Nature* **388,** 773–778
7. Kozak, K. R., Crews, B. C., Morrow, J. D., Wang, L. H., Ma, Y. H., Weinander, R., Jakobsson, P. J., and Marnett, L. J. (2002) Metabolism of the endocannabinoids, 2-arachidonylglycerol and anandamide, into prostaglandin, thromboxane, and prostacyclin glycerol esters and ethanolamides. *J. Biol. Chem.* **277,** 44877–44885
8. Rouzer, C. A., Tranguch, S., Wang, H., Zhang, H., Dey, S. K., and Marnett, L. J. (2006) Zymosan-induced glycerylprostaglandin and prostaglandin synthesis in resident peritoneal macrophages: roles of cyclo-oxygenase-1 and -2. *Biochem. J.* **399,** 91–99
9. Hu, S. S., Bradshaw, H. B., Chen, J. S., Tan, B., and Walker, J. M. (2008) Prostaglandin E_2 glycerol ester, an endogenous COX-2 metabolite of 2-arachidonoylglycerol, induces hyperalgesia and modulates NFκB activity. *Br. J. Pharmacol.* **153,** 1538–1549
10. Kozak, K. R., Rowlinson, S. W., and Marnett, L. J. (2000) Oxygenation of the endocannabinoid, 2-arachidonylglycerol, to glyceryl prostaglandins by cyclooxygenase-2. *J. Biol. Chem.* **275,** 33744–33749
11. Rowlinson, S. W., Crews, B. C., Lanzo, C. A., and Marnett, L. J. (1999) The binding of arachidonic acid in the cyclooxygenase active site of mouse prostaglandin endoperoxide synthase-2 (COX-2): a putative L-shaped binding conformation utilizing the top channel region. *J. Biol. Chem.* **274,** 23305–23310
12. Goodwin, D. C., Rowlinson, S. W., and Marnett, L. J. (2000) Substitution of tyrosine for the proximal histidine ligand to the heme of prostaglandin endoperoxide synthase 2: implications for the mechanism of cyclooxygenase activation and catalysis. *Biochemistry* **39,** 5422–5432
13. Marnett, L. J., Siedlik, P. H., Ochs, R. C., Pagels, W. R., Das, M., Honn, K. V., Warnock, R. H., Tainer, B. E., and Eling, T. E. (1984) Mechanism of the stimulation of prostaglandin H synthase and prostacyclin synthase by the antithrombotic and antimetastatic agent, nafazatrom. *Mol. Pharmacol.* **26,** 328–335
14. Funk, M. O., Isacc, R., and Porter, N. A. (1976) Preparation and purification of lipid hydroperoxides from arachidonic and γ-linolenic acids. *Lipids* **11,** 113–117
15. Kozak, K. R., Gupta, R. A., Moody, J. S., Ji, C., Boeglin, W. E., DuBois, R. N., Brash, A. R., and Marnett, L. J. (2002) 15-Lipoxygenase metabolism of 2-arachidonylglycerol: generation of a peroxisome proliferator-activated receptor α agonist. *J. Biol. Chem.* **277,** 23278–23286
16. Kulmacz, R. J., Miller, J. F., Jr., Pendleton, R. B., and Lands, W. E. (1990) Cyclooxygenase initiation assay for hydroperoxides. *Methods Enzymol.* **186,** 431–438
17. Jiang, Z. Y., Woollard, A. C., and Wolff, S. P. (1991) Lipid hydroperoxide measurement by oxidation of Fe^{2+} in the presence of xylenol orange: comparison with the TBA assay and an iodometric method. *Lipids* **26,** 853–856
18. Landino, L. M., Crews, B. C., Timmons, M. D., Morrow, J. D., and Marnett, L. J. (1996) Peroxynitrite, the coupling product of nitric oxide and superoxide, activates prostaglandin biosynthesis. *Proc. Natl. Acad. Sci. U.S.A.* **93,** 15069–15074
19. Hemler, M. E., and Lands, W. E. (1980) Evidence for a peroxide-initiated free radical mechanism of prostaglandin biosynthesis. *J. Biol. Chem.* **255,** 6253–6261
20. Kingsley, P. J., Rouzer, C. A., Saleh, S., and Marnett, L. J. (2005) Simultaneous analysis of prostaglandin glyceryl esters and prostaglandins by electrospray tandem mass spectrometry. *Anal. Biochem.* **343,** 203–211
21. Seiler, A., Schneider, M., Förster, H., Roth, S., Wirth, E. K., Culmsee, C., Plesnila, N., Kremmer, E., Rådmark, O., Wurst, W., Bornkamm, G. W., Schweizer, U., and Conrad, M. (2008) Glutathione peroxidase 4 senses and translates oxidative stress into 12/15-lipoxygenase dependent- and AIF-mediated cell death. *Cell Metab.* **8,** 237–248
22. Milne, G. L., Sanchez, S. C., Musiek, E. S., and Morrow, J. D. (2007) Quantification of F2-isoprostanes as a biomarker of oxidative stress. *Nat. Protoc.* **2,** 221–226
23. Dietz, R., Nastainczyk, W., and Ruf, H. H. (1988) Higher oxidation states of prostaglandin H synthase: rapid electronic spectroscopy detected two spectral intermediates during the peroxidase reaction with prostaglandin G_2. *Eur. J. Biochem.* **171,** 321–328
24. Tsai, A., Wei, C., Baek, H. K., Kulmacz, R. J., and Van Wart, H. E. (1997) Comparison of peroxidase reaction mechanisms of prostaglandin H synthase-1 containing heme and mangano protoporphyrin IX. *J. Biol. Chem.* **272,** 8885–8894
25. Strieder, S., Schaible, K., Scherer, H. J., Dietz, R., and Ruf, H. H. (1992) Prostaglandin endoperoxide synthase substituted with manganese protoporphyrin IX: formation of a higher oxidation state and its relation to cyclooxygenase reaction. *J. Biol. Chem.* **267,** 13870–13878
26. Wada, M., DeLong, C. J., Hong, Y. H., Rieke, C. J., Song, I., Sidhu, R. S., Yuan, C., Warnock, M., Schmaier, A. H., Yokoyama, C., Smyth, E. M., Wilson, S. J., FitzGerald, G. A., Garavito, R. M., Sui de, X., Regan, J. W., and Smith, W. L. (2007) Enzymes and receptors of prostaglandin pathways with arachidonic acid-derived *versus* eicosapentaenoic acid-derived substrates and products. *J. Biol. Chem.* **282,** 22254–22266
27. Malkowski, M. G., Thuresson, E. D., Lakkides, K. M., Rieke, C. J., Micielli, R., Smith, W. L., and Garavito, R. M. (2001) Structure of eicosapentaenoic and linoleic acids in the cyclooxygenase site of prostaglandin endoperoxide H synthase-1. *J. Biol. Chem.* **276,** 37547–37555
28. Vecchio, A. J., and Malkowski, M. G. (2011) The structural basis of endocannabinoid oxygenation by cyclooxygenase-2. *J. Biol. Chem.* **286,** 20736–20745
29. Sakamoto, H., Imai, H., and Nakagawa, Y. (2000) Involvement of phospholipid hydroperoxide glutathione peroxidase in the modulation of prostaglandin D_2 synthesis. *J. Biol. Chem.* **275,** 40028–40035